Revision #1

Word Count: 5799

The first occurrence of the carbide anion, C^{4-}, in an oxide mineral: Mikecoxite, ideally $(CHg_4)OCl_2$, from the McDermitt open-pit mine, Humboldt County, Nevada, U.S.A.

MARK A. COOPER[1], GAIL DUNNING[2], FRANK C. HAWTHORNE[1,*], CHI MA[3], ANTHONY R. KAMPF[4],
JOHN SPRATT[5], CHRISTOPHER J. STANLEY[5], AND ANDREW G. CHRISTY[6]

[1] Department of Geological Sciences, University of Manitoba, Winnipeg, Manitoba R3T 2N2, Canada

[2] Deceased

[3] Division of Geological and Planetary Sciences, California Institute of Technology, Pasadena, California 91125, USA

[4] Mineral Sciences Department, Natural History Museum of Los Angeles County, 900 Exposition Boulevard, Los Angeles, CA 90007, USA

[5] Department of Earth Sciences, Natural History Museum, London, SW7 5BD, United Kingdom

[6] Geosciences, Queensland Museum, 122 Gerler Road, Hendra, Qld 4011, and Christy Mineralogical Consulting, P.O. Box 517, Hamilton, Qld 4007, Australia.

* Corresponding author email: frank.hawthorne@umanitoba.ca

ABSTRACT

Mikecoxite, ideally $(CHg_4)OCl_2$, is the first mercury-oxide-chloride-carbide containing a C^{4-} anion coordinated by four Hg atoms (a permercurated methane derivative) to be described as a mineral species. It was found at the McDermitt open-pit mine on the eastern margin of the McDermitt Caldera, Humboldt County, Nevada, USA. It is monoclinic, space group $P2_1/n$, Z = 4; *a* 10.164(5), *b* 10.490(4), *c* 6.547(3) Å, *V* 698.0(5) Å^3. Chemical analysis by electron microprobe gave Hg 86.38, Cl 11.58, Br 0.46, C 1.81, sum = 100.23 wt%, and O was detected but the signal was too weak for quantitative chemical analysis. The empirical formula, calculated on the basis of Hg + Cl + Br = 6 apfu, is $(C_{1.19}Hg_{3.39})(Cl_{2.57}Br_{0.05})_{\Sigma 2.62}$, and the ideal formula based on the chemical analysis and the crystal structure is $(CHg_4)OCl_2$. The seven strongest lines in the X-ray powder diffraction pattern are [*d* (Å)(*I*)(*hkl*)]: 2.884, 100, (230); 2.989, 81, (–301, 301, –112, 112, –131, 131); 2.673, 79, (–122, 122, –212, 212); 1.7443, 40, (060, –432, 432); 5.49, 34, (–101, 101); 4.65, 32, (120); 2.300, 30, (–312, 312). The Raman spectrum shows three bands at 638, 675 and 704 cm^{-1}, well above the range characteristic of NHg_4 stretching vibrations that occur between 540 and 580 cm^{-1}, that are assigned to CHg_4 stretching vibrations. Mikecoxite forms intergrowths of bladed crystals up to 100 µm long that occur on granular quartz or in vugs associated with kleinite. It is black with a submetallic to metallic luster and strong specular reflections, and does not fluoresce under short- or long-wave ultraviolet light. Neither cleavage nor parting were observed, and the calculated density is 8.58 g/cm^3. In the crystal structure of mikecoxite, $(C^{4-}Hg^{2+}{}_4)$ groups link through O^{2-} ions to form three-membered rings that polymerize into corrugated $[CHg_4OCl]^+$ layers with near-linear C^{4-}–Hg^{2+}–O and C^{4-}–Hg^{2+}–Cl linkages. The layers link in the third direction directly via weak Hg^{2+}–O^{2-} and Hg^{2+}–Cl^- bonds to adjacent layers and also indirectly via interlayer Cl^-. A bond-valence parameter has

been derived for (Hg^{2+}–C^{4-}) bonds: $R_o = 2.073$ Å, $b = 0.37$, and this gives bond-valence sums at the C^{4-} ions in accord with the valence-sum rule. The source of carbon for mikecoxite in the volcanic high-desert environment of the type locality seems to be methane, with the reaction catalyzed by microbiota through full mercuration of carbon atoms, beyond the first stage that produces the volatile and highly mobile methylmercury, $[CH_3Hg]^+$, a potent neurotoxin that accumulates in marine food chains.

Both the mineral and the mineral name have been approved by the Commission on New Minerals, Nomenclature and Classification of the International Mineralogical Association (IMA 2021–060). The mineral is named after Michael F. Cox (b. 1958), a founding member of the New Almaden Quicksilver County Park Association (NAQCPA) who was responsible for characterizing and remediating environmental mercury on site, and who recovered the rock containing the new mineral.

Keywords: Mikecoxite, new mineral, mercury-oxide-chloride-carbide, crystal-structure refinement, Raman spectrum, electron-microprobe analysis, McDermitt open-pit mine, Humboldt County, Nevada, USA.

INTRODUCTION

As part of our continuing interest in Hg-bearing minerals (Hawthorne et al. 1994; Cooper and Hawthorne 2003, 2009; Cooper et al. 2013, 2016, 2019; Roberts et al. 2001, 2002, 2003a,b, 2004, 2005), here we report on a new mercury-oxide-chloride-carbide mineral from the McDermitt mine. The new mineral is named after Mr. Michael F. Cox (born 1958) of Soquel, California, who recovered the rock containing the new mineral. Michael Cox has had a life-long interest in Hg minerals. Most notably, he was a founding member of the New Almaden Quicksilver County Park Association (NAQCPA), was responsible for characterizing and remediating environmental mercury on site, and contributed substantially to the creation of a world-class mercury-mining interpretive center in New Almaden, California. He also contributed substantially to the late Gail Dunning's search for interesting new mercury minerals (Dunning et al. 2019).

One holotype specimen (rock piece, single-crystal mount, polished mount used for C analysis) and one cotype specimen (used for the Raman and PXRD studies) are deposited in the collections of the Natural History Museum of Los Angeles County, Los Angeles, California, USA, catalogue numbers 76196 and 76197, respectively.

OCCURRENCE

Mikecoxite was found in a single rock sample from the central floor region of the McDermitt open-pit mine, situated along the eastern margin of the McDermitt Caldera, Humboldt County, Nevada, USA (41°55'11.5"N 117°48'45.8"W). The McDermitt Caldera is a Miocene volcanic structure (16.6 – 15.7 Ma) along the SW-NE trend of Yellowstone-type volcanogenic-hydrothermal features associated with movement of the continental plate over the

Yellowstone hot spot. Further details of the geologic setting and of the McDermitt mine history are given in Dunning et al. (2019) and references therein. The McDermitt mine was the single largest North American mercury producer in the 1980s, extracting mercury ore from a ~ 670 x 760 m open pit. The primary mercury minerals are cinnabar and corderoite in argillized Miocene tuffaceous lacustrine sediments overlying a paleo lake bed of silicified volcaniclastic breccia. The identification of the new mercury-sulfide-chloride mineral corderoite as a supplementary ore mineral was noted by Foord et al. (1974). Mining ceased in 1990 at the McDermitt mine. Mikecoxite was discovered in a loose cobble from a central location of the pit floor (Area 2; Dunning et al. 2019), recovered during a mineral-collecting trip in 2015. Area 2 consists of exposed silicified and brecciated volcanic tuffs, with remnants of a capping fluvial tuffaceous horizon that is also silicified. The mikecoxite-bearing cobble seems consistent with it originating from the latter horizon. The overlying lacustrine sediments have been removed. Abundant kleinite and terlinguacreekite occur with lesser calomel and eglestonite, coating fractures and in quartz-lined cavities within these silicified units in Area 2. Mikecoxite was discovered in a single vug together with terlinguacreekite and kleinite, all crystallized on a quartz lining. A localized monoclinal structure is proposed for Area 2 with the lower silicified tuff (containing the kleinite-terlinguacreekite-mikecoxite assemblage) overlain by a bleached crumbly clay-rich tuff. Graded iron-stained horizons are also evident in Area 2. This distinction between an upper altered clay-rich horizon and lower silicified zone signifies an interface between differing fluid environments, with the monoclinal structure likely acting as a local trap.

The current-day Yellowstone Caldera is characterized by a more active margin containing a complex gas assemblage that includes H_2S, CH_4 and NH_3 (Sheppard et al. 1992). A similar mix of volatiles is consistent with the mercury nitride-carbide occurrence at the

McDermitt mine, located along the eastern margin of the McDermitt Caldera. Methane and ammonia trapped locally together with mercury and chlorine complexes may have led to formation of the mercury nitrides (kleinite, terlinguacreekite) and mercury-oxide-chloride-carbide (mikecoxite) via progressive substitution of Hg^{2+} complexes for hydrogen in precursor NH_3 (or NH_4^+) and CH_4. A microbial presence may have promoted electrophilic attack of the N–H and C–H bonds, such that H was displaced by Hg-anion complexes, leading to $(NHg_4)^{5+}$ and $(CHg_4)^{4+}$ groups in the mercury minerals discovered. The sulfur and halogen content of circulating vapors and fluids is known to affect chemical speciation of Hg^{2+}, and increased anaerobic microbial activity is thought to enhance methylation of Hg, i.e., conversion of CH_4 to $(CH_3Hg)^+$; in addition, available Fe^{2+} may have scavenged S^{2-} and formed iron sulfides (e.g., pyrite), allowing higher activity of Hg^{2+} complexes in solution and increasing bioavailability of Hg^{2+} for methylation (Bravo and Cosio 2020). The synthetic polymer Hofmann's Base, $(CHg_4)O(H_2O)(OH)_2$, similar to mikecoxite in chemical composition and probably in structure (see below), is formed abiotically by reaction of HgO with ethanol under alkaline conditions. However, as no obvious organic matter that would contain alcohol groups is seen in close association with mikecoxite, CH_4 is presumed to be the source of the C. This, or microbial metabolites of it, may have reacted with hydroxyl- and chloro-mercury complexes, in the presence of a microbial catalyst, to form this unusual mineral.

PHYSICAL PROPERTIES

Black bladed crystals of mikecoxite (Fig. 1a) form concentrations on granular quartz and also occur in vugs associated with pale-orange vitreous kleinite (Fig. 1b) and terlinguacreekite. Individual crystals are up to 0.1 mm long, are opaque and have submetallic to metallic luster and strong specular reflections, and neither cleavage nor parting were observed. Hardness was not determined but the crystals were soft when manipulated with a needle. Mikecoxite does not fluoresce under short- or long-wave ultraviolet light. Crystals are not suitable for reflectance measurements due to strong internal reflections. The calculated density is 8.58 g/cm^3 using the ideal chemical formula and the cell dimensions derived from single-crystal X-ray diffraction. The *a:b:*c ratio calculated from the single-crystal unit-cell parameters is 0.9689:1:0.6241.

RAMAN SPECTROSCOPY

Raman spectroscopy was done on a Horiba XploRA PLUS using a 785 nm diode laser, a 200 μm slit, a 1800 gr/mm diffraction grating and a 100× (0.9 NA) objective. Spectra recorded from crystals in varying orientations show significant variation in band intensities. Figure 2 shows two spectra, one recorded with the laser approximately perpendicular to a flat lustrous face, probably (010), and one with the laser approximately perpendicular to an irregular stepped face, probably (100). Only the 800 to 60 cm^{-1} range is shown because the spectra are featureless from 2000 to 800 cm^{-1}. Tentative band assignments based on Mink et al. (1983) and Cooper et al. (2013) are shown. The spectrum shows three bands at 638, 675 and 704 cm^{-1}, well above the range characteristic of NHg_4 stretching vibrations that occur between 540 and 580 cm^{-1} (Cooper et al. 2013, 2019). As Hg^{2+}–C^{4-} bonds are significantly stronger than Hg^{2+}–N^{3-} bonds (bond strengths of 1.00 versus 0.75 v.u.), CHg_4 stretching vibrations should occur at wavenumbers significantly higher than those for NHg_4 groups, supporting the assignment of the bands at 638, 675 and 704 cm^{-1} as CHg_4 stretching vibrations.

CHEMICAL COMPOSITION

Electron-microprobe analysis (18 points) was done at the Natural History Museum (London) using a Cameca SX100 electron microprobe in WDS mode for the elements Hg, Cl, Br (F, S and I were below detection). Analytical conditions were 10 kV accelerating voltage, 4 nA beam current and 1 μm beam diameter. Preliminary WDS scans at Caltech using an LDE2 crystal indicated the presence of C and absence of N, and analysis for C (3 points) was done at Caltech on a JEOL 8200 electron microprobe in WDS mode. The presence of O is also indicated by a very weak peak in wavelength scans in the electron microprobe using LDE1 and LDE2 crystals (Fig. 3) but the peak intensity is too weak for quantification. Analytical conditions were 10 kV accelerating voltage, 10 nA beam current and 5 μm beam diameter. No suitable mercury-carbide standard was available; chemical grade Hg-acetate was used as it provides a quantitative source of C within a Hg matrix. A 1 nm thick Ir coating was applied to the surface of the sample and Hg-acetate standard prior to analysis for C. Mikecoxite was very sensitive to the electron beam during both sessions, and we attribute the poor quality of the chemical data to a combination of sample / standard instability and general mismatching of sample and standard with respect to the differing bonding environments of C. We regard the experimental compositional data as independently supporting the proposed formula and the chemical formula calculated from the high-quality fully ordered structure-refinement; thus, the simplified formula given here is derived from the structure formula. Analytical data are given in Table 1. The empirical formula calculated on the basis of Hg + Cl + Br = 6 is $(C_{1.19}Hg_{3.39})(Cl_{2.57}Br_{0.05})_{\Sigma 2.62}$. The structure formula based on the crystal-structure refinement is $(CHg_4)O(Cl_{1.958}Br_{0.042})_{\Sigma 2}$. The simplified formula is $(CHg_4)O(Cl,Br)_2$ and the ideal formula is $(CHg_4)OCl_2$, which requires C 1.33, Hg 89.02, O 1.78, Cl 7.87, total 100 wt%.

X-RAY POWDER DIFFRACTION

Powder X-ray diffraction (PXRD) data were collected using a Rigaku R-Axis Rapid II curved-imaging-plate microdiffractometer with monochromatized Mo*K*α radiation. A Gandolfi-like motion on the φ and ω axes was used to randomize the sample. Observed *d* values and intensities were derived by profile fitting using JADE Pro software (Materials Data, Inc.). Data are given in Table 2. Note that the relative weakness of the PXRD and the high background did not allow refinement of the cell parameters by whole-pattern fitting; however, whole-pattern fitting using the single-crystal cell provided an almost perfect fit to the observed data.

SINGLE-CRYSTAL X-RAY DATA COLLECTION

Crystals of mikecoxite occur as interpenetration twins (2-fold rotation about the **c**-axis). A suspected twin aggregate was trimmed down in size and a small fragment mounted on a MiTeGen polymer tip. The crystal was mounted on a Bruker D8 three-circle diffractometer equipped with a rotating-anode generator (Mo*K*α radiation), multilayer optics and an APEX-II detector. Although the crystal was later discovered during structure refinement to be a near-merohedral twin, its uniform diffraction spots did not exhibit any evidence of the presence of more than one crystal. Using 30 s frames with a 0.3° frame width, a highly redundant data set (> 11 x redundancy) was collected with a total of 23,355 integrated reflections. Significant data oversampling allowed robust empirical modelling of X-ray absorption for this extreme absorber (mμ = 88.59 mm^{-1}). The unit-cell dimensions were obtained by least-squares refinement of 4073 reflections with $I_o > 10\sigma I$. Empirical absorption corrections (SADABS; Sheldrick 2008) were applied and equivalent reflections were merged. Pertinent details are listed in Table 3.

CRYSTAL-STRUCTURE SOLUTION AND REFINEMENT

Initially, the single-crystal diffraction data seemed to conform with an approximately orthogonal unit-cell with a = 10.49, b = 6.55, c = 10.16 Å, and general extinction conditions indicated space group *Pnma*. The structure was solved by direct methods in *Pnma* and refined to an R_1 index of 2.7%. Although the refined structure model seemed quite reasonable, several reflections violated the extinction conditions for space group *Pnma*: ($hk0$) reflections with $h \neq 2n$ and $k = 2n$ were observed in the range 10–30 $F_o > \sigma F$. Additionally, the anisotropic-displacement behavior of the C atom was less than ideal. These observed reflections are inconsistent with the presence of an *a*-glide plane perpendicular to the **c**-axis (10.16 Å). To further investigate these violating reflections, simulated precession slices were generated from the raw data frames. The suspect reflections were clearly present on the *hk*0 slice, and also appeared consistent with *mm* Laue symmetry within the slice. The conditions for all observed reflections are: ($0kl$): $k + l = 2n$; ($h00$): $h = 2n$; ($0k0$): $k = 2n$; ($00l$): $l = 2n$, which are collectively inconsistent with all orthorhombic space groups. For the current cell choice, the diffraction symmetry seemed consistent with monoclinic symmetry, **a**-axis unique, ($P2_1/n11$). The diffraction data were then carefully inspected for subtle signs of underlying monoclinic symmetry; i.e., possible metric deviation of the refined unit-cell angles from 90°, and possible Laue symmetry lower than *mmm*. The unconstrained unit-cell parameters refined to a = 10.490 (4), b = 6.547 (3), c = 10.164 (5) Å, α = 90.037 (10), β = 90.000 (18), γ = 89.985 (9)°. The α angle shows the largest deviation from 90°. The Laue merging (R_{merge}) in $2/m$ for each unique axis choice is: **a** (0.9%), **b** (1.2%), **c** (1.2%), and for *mmm* symmetry (1.3%). Although monoclinic character is not overly convincing from these results alone, the metric deviation from orthogonal axes and the Laue merging results collectively support the best choice as monoclinic with **a** as the unique axis. This selection, combined with the analysis of the simulated precession slices, suggests the space group $P2_1/n$. The cell was re-oriented and the final monoclinic-constrained unit-cell parameters are a = 10.164 (5), b = 10.490 (4), c = 6.547 (3) Å, β = 90.037 (10)°. The crystal structure was refined in $P2_1/n$ to an R_1 index of 3.3 %; however, the worst-fit reflections all had $F_o >> F_c$, characteristic of twinning. A twin instruction (–1 0 0 0 –1 0 0 0 1) consistent with a 2-fold rotation twin-axis along **c** was inserted into the refinement, and the final model refined to R_1 = 1.8 % with a 0.474(2) near-merohedral twin-fraction. The lower R_1 value and improved anisotropic-displacement behavior of the C atom in the $P2_1/n$ structure model (which now includes all observed data) establish mikecoxite as monoclinic with space group $P2_1/n$. Four Hg sites refined to full occupancy by Hg. Two Cl sites were refined as Cl; one Cl site showed slight excess scattering and was modelled as Cl + Br with the refined site content of Br close to the Br content measured by EMPA (0.46 wt% Br, Table 1). Two sites were designated as fully occupied by O and C (this assignment is discussed later in more detail). Data collection and refinement details are given in Table 3, atom coordinates and displacement parameters in Table 4 and selected bond distances and angles in Table 5. A table of structure factors and a Crystallographic Information File (CIF) for mikecoxite have been deposited on the MSA website.

THE $(C^{4-}Hg^{2+}_4)^{4+}$ GROUP

The occurrence and characterization of a $(C^{4-}Hg^{2+}_4)^{4+}$ group warrants detailed discussion as in previously known minerals the C^{4-} anion occurs only in moissanite, SiC, and is rare in synthetic inorganic structures in general. The other carbides known as minerals are metallic phases with substantial metal-metal bonding and interstitial carbon of indeterminate valence state. However, electroneutrality in mikecoxite, $(CHg_4)OCl_2$, requires that the carbon be a C^{4-} anion. The four Hg sites in mikecoxite are fully occupied by Hg^{2+}; Hg^{1+} invariably occurs as $[Hg^+–Hg^+]$ dimers with Hg–Hg distances of ~ 2.53 Å [e.g., magnolite (Grice 1989), hanawaltite (Grice 1999), vasililyevite (Cooper and Hawthorne 2003), tedhadleyite (Cooper and Hawthorne 2009)], and this arrangement was not present in the structure. In crystal structures containing Hg^{2+}, there is an anticipated near-linear $[anion–Hg^{2+}–anion]$ configuration with relatively short strong bonds between Hg^{2+} and the associated anions. In all Hg^{2+} bearing minerals examined thus far, the anions linked to Hg^{2+} are N^{3-}, O^{2-}, S^{2-}, Cl^-, Br^- and I^-. In mikecoxite, one anion bonded to each of the four crystallographically distinct Hg^{2+} cations is a C^{4-} anion. Such anion-centered tetrahedra are relatively common in minerals (Krivovichev et al. 2013; Hawthorne 2014), particularly $(O^{2-}Cu^{2+}{}_4)$, $(O^{2-}Pb^{2+}{}_4)$, $(O^{2-}Hg^{2+}{}_4)$ and $(N^{3-}Hg^{2+}{}_4)$. However, the C^{4-} anion had not been found bonded to Hg^{2+} in a mineral prior to the discovery of mikecoxite, and as the latter occurs with kleinite and terlinguacreekite, both containing $(N^{3-}Hg^{2+}{}_4)$ groups (Cooper et al. 2013), characterization of the C^{4-} anion is of particular importance. The chemical-analytical data for C in mikecoxite was acquired after the final interpretation of the crystal structure. There are four criteria arising from the refinement that are indicative of atom identity: (1) the relative magnitude of the refined site-scattering; (2) the interatomic distances to bonded atoms; (3) coordination number; (4) the requirement for electroneutrality of the structure.

Refined C-site scattering

As a general rule, structural sites with low-coordination numbers are fully occupied, a result of the valence-sum rule (Brown 2016; Hawthorne 2012, 2015). If a tetrahedrally coordinated site is fully occupied by a single scattering species, then the correct scattering factor will refine to an occupancy of ~1.0, and any incorrect scattering factor will refine to an occupancy significantly different from 1.0. For mikecoxite, the atoms potentially bonded to Hg^{2+} are the light scatterers O, N and C (with $Z = 8$, 7 and 6, respectively) and the medium-strength scatterers S and Cl ($Z = 16$ and 17, respectively). For the anions coordinating the four Hg sites in mikecoxite, initial anion site-scattering assessment revealed two configurations: (1) X–Hg–X; and (2) X–Hg–Y, where X is a light scatterer ($Z = 8$, 7 and 6) and Y is a medium-strength scatterer ($Z = 16$ and 17).

For mikecoxite specifically, extreme oversampling during data collection for a small crystal resulted in rigorous determination of the empirical absorption correction. The resulting high-quality structure refinement allowed accurate discrimination of such scattering differences because systematic error from absorption effects had been almost completely eliminated. There are two crystallographically distinct light-anion sites (currently labelled L1 and L2). For both sites, the site occupancies were refined independently with each of the scattering factors for C, N and O, and freely refining anisotropic-displacement parameters. The resulting refined occupancies for the two sites are as follows: $^{L1}(C_{1.68(3)}, N_{1.32(2)}$ and $O_{1.07(2)})$ and $^{L2}(C_{1.02(3)}, N_{0.79(2)}$ and $O_{0.63(2)})$. The differing refined site-occupancies are compelling support for L1 = O and L2 = C, and the respective anions were so assigned. This test was vital in reliably establishing that the L2 site is occupied by C and not N in mikecoxite, as this anion site is tetrahedrally coordinated by four Hg atoms with bond lengths *and* coordination compatible with either N^{3-} or C^{4-} as the anion, leaving the site-scattering difference as the only direct structure-refinement criterion available to make the distinction. The O site is coordinated by three proximal (and two distal) Hg atoms, compatible with O^{2-}; such a coordination is not expected for either N^{3-} or C^{4-} anions based on a survey of other mercury structures.

Interatomic distances

There are four Hg sites in mikecoxite, with strong axial C–Hg–O and C–Hg–Cl bonds, in addition to weaker equatorial bonds to distant O and Cl anions (Fig. 4). For configuration (2): X–Hg–Y, the Hg–Y distance of 2.36 Å indicates that Y is Cl (the presence of Cl was later substantiated by chemical analysis).

The C^{4-} anion is tetrahedrally coordinated by four Hg^{2+} cations, and the O^{2-} anion by three proximal and two distal Hg^{2+} cations (Table 5, Fig. 5a,b). The refined C–Hg distances of 2.054–2.093 Å fall within the range 2.04–2.11 Å observed in synthetic compounds with (CHg_4) groups (Milić et al. 2009). Moreover, the <C–Hg> distance of 2.073 Å in mikecoxite is nearly identical to the grand <N–Hg> distance of 2.072 Å for the ten well-refined (NHg_4) groups in gaildunningite (Cooper et al. 2019). As we are not aware of any published bond-valence parameters for the C^{4-}–Hg^{2+} bond, we propose here the values $R_o = 2.073$, $b = 0.37$ based on the well-refined C–Hg distances in mikecoxite. This provides a bond-valence sum of 4.00 v.u. for the C atom, and in turn provides a measure of the bond-valence received by the Hg^{2+} cation from the C^{4-} anion (Fig. 5a). The three strong bonds formed between the O^{2-} anion and coordinating Hg^{2+} cations range from 2.080–2.114 Å (Table 5), and are all slightly longer than the <O–Hg> distance of ~ 2.07Å for O^{2-} coordinated by only three Hg^{2+} cations (Cooper et al. 2013). However, the O^{2-} anion in mikecoxite also receives two additional weaker bonds from more distant Hg^{2+} cations. The resulting bond-valence sum of 2.02 v.u. for the O^{2-} anion [using Hg^{2+}–O^{2-} bond-valence parameters of Brese and O'Keefe (1991); Cooper et al. (2013)] from all five bonds to Hg^{2+} supports [5]-coordination of this anion (Fig. 5b). The bond-valence sums for the four Hg sites range from 1.81 to 1.94 v.u. using the Brese and O'Keefe (1991) parameters for

Hg^{2+}–Cl^- bonds. The bond-valence sum at the Cl1 anion is 1.01 v.u., and 0.45 v.u. at the Cl2 anion that occupies a void and forms eight longer bonds (3.058–3.512 Å) to neighboring Hg^{2+} cations. Some degree of positional disorder is often associated with the more loosely bound halogens in Hg^{2+} structures, and the bond-valence sums for both the Hg^{2+} cations and these halogens are not generally ideal.

BOND TOPOLOGY

Three (CHg_4) tetrahedra link via bridging O atoms to form triangular rings that further link to form layers of composition $[CHg_4OCl]^+$ parallel to (010) (Fig. 6a). The fourth vertex of the (CHg_4) tetrahedron (not involved in layer connectivity) contains a strongly bonded terminal Cl^- anion that alternately projects above and below the layer. This layer carries a 1+ charge, and is distinctly corrugated, with an additional charge-balancing Cl^- between layers (Fig. 6b). Weaker equatorial bonds extend from Hg^{2+} to O^{2-} and Cl^- in adjacent layers and to the interlayer Cl^-, linking the layers into a three-dimensional structure.

RELATION TO OTHER STRUCTURES

Mikecoxite, a mercury-oxide-chloride-carbide mineral containing a C atom coordinated by four Hg atoms (a permercurated methane derivative), is the first of its kind as a mineral species. This unexpected result is supported by (1) the refined scattering at the C site, (2) the presence of a C peak in the electron microprobe analysis, (3) the lack of an Hg–N peak in the Raman spectrum, (4) the satisfaction of the valence-sum rule at the C site for occupancy by C^{4-}, and (5) the electroneutrality of the overall structure.

There are only a few synthetic structures known that contain a (CHg_4) group, and only one of these, $(CHg_4)(OH)(H_2O)_2](CF_3SO_3)_3(H_2O)$, is polymeric, containing (CHg_4) groups linked via strong –Hg–OH–Hg– linkages to form chains (Milić et al. 2009). The (CHg_4) group stereochemically resembles the tetrahedral (NHg_4) group that has been described in several mercury-halide-nitride minerals (e.g., gaildunningite, comancheite, gianellaite, kleinite, mosesite). Mercury nitrides containing $–N^{3–}–Hg^{2+}–N^{3–}–$ bridges tend to freely polymerize, whereas mercury carbides are unlikely to polymerize via $–C^{4–}–Hg^{2+}–C^{4–}–$ bridges due to the relative difference in incident bond-valence at Hg^{2+}. The $Hg^{2+}–N^{3–}$ bond has a bond valence of ~0.75 v.u., whereas the $Hg^{2+}–C^{4–}$ bond has a bond valence of ~1.0 v.u., which results in an incident bond-valence of 1.5 v.u. at Hg^{2+} for a $–N^{3–}–Hg^{2+}–N^{3–}–$ bridge, and 2.0 v.u. for a $–C^{4–}–Hg^{2+}–C^{4–}–$ bridge. The Hg^{2+} coordination commonly includes weak equatorial bonds approximately orthogonal to the near-linear (anion)-Hg^{2+}-(anion) axis. The bond-valence deficiency of 0.5 v.u. at the Hg^{2+} atom in a $–N^{3–}–Hg^{2+}–N^{3–}–$ bridge allows that additional equatorial-anion interaction, whereas the incident bond-valence of 2.0 v.u. at Hg^{2+} in a $–C^{4–}–Hg^{2+}–C^{4–}–$ bridge precludes such an interaction. Synthetic Hg-carbides with refined structures are generally monomeric, containing $C(Hg–X)_4$ groups (X = an anion group) with only weak intermolecular bonding. Polymerization of (CHg_4) groups in mikecoxite occurs via incorporation of bridging $O^{2–}$ anions that reduce the overall bond-valence contributed to the neighboring Hg^{2+} ion and allow additional weak equatorial bonds. The bridging $(OH)^-$ anion in synthetic $[CHg_4(OH)(H_2O)_2](CF_3SO_3)_3(H_2O)$ facilitates simple –Hg–OH–Hg– linkage between two neighboring (CHg_4) groups, forming linear chains. The only compound thought to contain an $O^{2–}$ anion that bridges three (CHg_4) groups is Hofmann's Base, $(CHg_4)O(H_2O)(OH)_2$, which is of unknown structure but is thought to contain a tetramercuriomethane-oxide layer (Milić et al. 2009) that is topologically similar to that in mikecoxite. Mikecoxite is the first mineral known to contain a (CHg_4) group, and also the first direct structural evidence supporting the tetramercuriomethane-oxide layer topology of Hofmann's Base.

IMPLICATIONS

Mikecoxite is the first discovery of dissolved Hg^{2+} reacting with organic compounds in nature to form an insoluble crystalline solid. The source of carbon for mikecoxite in the volcanic high-desert environment of the type locality appears to be methane, with the reaction catalyzed by microbiota. However, the chemical and likely structural similarity between mikecoxite and Hoffman's Base suggests that the mineral could also form by a mechanism similar to that which produces Hoffman's Base in the laboratory: attack by $[HgOH]^+$ ions on the terminal methyl group of a beta ketone or alcohol under alkaline conditions. Such functional groups in organic humate polymers could produce mikecoxite on reaction of these abundant soil constituents with alkaline saline groundwater containing Hg^{2+}, even in the absence of catalytic microbes. Chlorine in treated water is known to react with humate to produce chloroform by the analogous haloform reaction (Reckhow et al. 1990).

The existence of mikecoxite at the type locality shows that appropriate microbes can achieve immobilization of mercury through full mercuration of carbon atoms, beyond the first stage that produces the volatile and highly mobile methylmercury, $[CH_3Hg]^+$, a potent neurotoxin that is known to accumulate in marine food chains (cf. Villar et al. 2020). This possibility suggests a novel way to immobilize mercury for environmental remediation.

ACKNOWLEDGEMENTS

We thank the reviewers for their comments. Financial support for this work came from the Natural Sciences and Engineering Research Council of Canada in the form of a Canada Research Chair in Crystallography and Mineralogy, and a Discovery grant to FCH, and by Canada Foundation for Innovation grants to FCH.

REFERENCES

Bravo, A.G., and Cosio, R.L. (2020) Biotic formation of methylmercury: A bio-physico-chemical conundrum. Limnology and Oceanography, 65, 1010–1027.

Brese N.E., and O'Keeffe M. (1991) Bond-valence parameters for solids. Acta Crystallographica, B47, 192–197.

Brown, I.D. (2016) The Chemical Bond in Inorganic Chemistry. The Bond Valence Model. 2nd Edition. Oxford University Press, U.K.

Cooper, M.A., and Hawthorne, F.C. (2003) The crystal structure of vasilyevite, $(Hg_2)^{2+}{}_{10}O_6I_3(Br,Cl)_3(CO_3)$. Canadian Mineralogist, 41, 1173–1181.

Cooper, M.A., and Hawthorne, F.C. (2009) The crystal structure of tedhadleyite, $Hg^{2+}Hg^{1+}{}_{10}O_4I_2(Cl,Br)_2$, from the Clear Creek Claim, San Benito County, California. Mineralogical Magazine, 73, 227–234.

Cooper, M.A., Abdu, Y.A., Hawthorne, F.C., and Kampf, A.R. (2013) The crystal structure of comancheite, $Hg^{2+}{}_{55}N^{3-}(OH,NH_2)_4(Cl,Br)_{34}$, and crystal-chemical and spectroscopic discrimination of N^{3-} and O^{2-} anions in Hg^{2+} compounds. Mineralogical Magazine, 77, 3217–3237.

Cooper, M.A., Abdu, Y.A., Hawthorne, F.C., and Kampf, A.R. (2016) The crystal structure of gianellaite, $[(NHg_2)_2](SO_4)(H_2O)_x$, a framework of (NHg_4) tetrahedra with ordered (SO_4) groups in the interstices. Mineralogical Magazine, 80, 869–875.

Cooper, M.A., Hawthorne, F.C., Roberts, A.C., Stanley, C.J., Spratt, J., and Christy, A.G. (2019) Gaildunningite, ideally $Hg^{2+}{}_3[NHg^{2+}{}_2]_{18}(Cl,I)_{24}$, a new mineral from the Clear Creek Mine, San Benito County, California, USA: Description and crystal structure. Canadian Mineralogist, 57, 295–310.

Dunning, G.E., Cox, M.F., Christy, A.G., Hadley, T.A., and Marty, J. (2019) Geology, mining history, mineralogy, and paragenesis of the McDermitt caldera complex, Opalite mining district, Humboldt county, Nevada, and Malheur county, Oregon. Baymin Journal, 20(4), 165 pp. www.baymin.org.

Foord, E.E., Berendsen, P., and Storey, L.O. (1974) Corderoite, first natural occurrence of α–$Hg_3S_2Cl_2$, from the Cordero mercury deposit, Humboldt County, Nevada. American Mineralogist, 59, 652–655.

Grice, J.D. (1989) The crystal structure of magnolite, $Hg^{+}{}_2Te^{4+}O_3$. Canadian Mineralogist, 27, 133–136.

Grice, J.D. (1999) Redetermination of the crystal structure of hanawaltite. Canadian Mineralogist, 37, 775 –778.

Hawthorne F.C. (2012) A bond-topological approach to theoretical mineralogy: crystal structure, chemical composition and chemical reactions. Physics and Chemistry of Minerals, 39, 841–874.

Hawthorne, F.C. (2014) The Structure Hierarchy Hypothesis. Mineralogical Magazine, 78, 957–1027.

Hawthorne F.C. (2015) Toward theoretical mineralogy: a bond-topological approach. American Mineralogist, 100, 696–713.

Hawthorne, F.C., Cooper, M., and Sen Gupta, P.K. (1994) The crystal structure of pinchite, $Hg_5Cl_2O_4$. American Mineralogist, 79, 1199–1203.

Krivovichev, S.V., Mentré, O., Siidra, O.I., Colmont, M., and Filatov, S.K. (2013) Anion-centered tetrahedra in inorganic compounds. Chemical Reviews, 113, 6459–6535.

Milić, D., Soldin, Ž., Giester, G., Popović, Z., and Matković-Čalogović, D. (2009) Crystal structure of the first polymeric tetramercurated methane derivative of Hofmann's Base. Croatica Chemica Acta, 82, 337–344.

Mink, J., Meić, Z., Gál, M., and Korpar-Čolig, B. (1983) Infrared, Raman and force field studies of tetrakis (anionomercuri) methanes. Journal of Organometallic Chemistry, 256, 203–216.

Reckhow, D.A., Singer, P.C., and Malcolm, R.L. (1990) Chlorination of humic materials: byproduct formation and chemical interpretations. Environmental Science & Technology, 24, 1655–1664.

Roberts, A.C., Groat, L.A., Raudsepp, M., Ercit, T.S., Erd, R.C., Moffatt, E.A., and Stirling, J.A.R. (2001) Clearcreekite, a new polymorph of $Hg^{1+}_3(CO_3)(OH)\cdot 2H_2O$, from the Clear Creek Claim, San Benito County, California. Canadian Mineralogist, 39, 779–784.

Roberts, A.C., Cooper, M.A., Hawthorne, F.C., Criddle, A.J., Stirling, J.A.R., and Dunning, G.E. (2002) Tedhadleyite, $Hg^{2+}Hg^{1+}_{10}O_4I_2(Cl,Br)_2$, a new mineral species from the Clear Creek claim, San Benito County, California. Canadian Mineralogist, 40, 909–914.

Roberts, A.C., Cooper, M.A., Hawthorne, F.C., Gault, R.A., Grice, J.D., and Nikischer, A.J. (2003a) Artsmithite, a new Hg^{1+}–Al phosphate-hydroxide from the Funderburk Prospect, Pike County, Arkansas, U.S.A. Canadian Mineralogist, 41, 721–725.

Roberts, A.C., Cooper, M.A., Hawthorne, F.C., Stirling, J.A.R., Paar, W.H., Stanley, C.J., Dunning, G.E., and Burns, P.C. (2003b) Vasilyevite, $(Hg_2)^{2+}_{10}O_6I_3Br_2Cl(CO_3)$, a new mineral species from the Clear Creek claim, San Benito County, California. Canadian Mineralogist, 41, 1167–1172.

Roberts, A.C., Stirling, J.A.R., Criddle, A.J., Dunning, G.E., and Spratt, J. (2004) Aurivilliusite, $Hg^{2+}Hg^{1+}OI$, a new mineral species from the Clear Creek claim, San Benito County, California, USA. Mineralogical Magazine, 68, 241–245.

Roberts, A.C., Gault, R.A., Paar, W.H., Cooper, M.A., Hawthorne, F.C., Burns, P.C., Cisneros, S., and Foord, E.E. (2005) Terlinguacreekite, $Hg^{2+}{}_3O_2Cl_2$, a new mineral species from the Perry pit, Mariposa Mine, Terlingua mining district, Brewster County, Texas, U.S.A. Canadian Mineralogist, 43, 1055–1060.

Sheppard, D.S., Truesdell A.H., and Janik, C.J. (1992) Geothermal gas compositions in Yellowstone National Park, USA. Journal of Volcanology and Geothermal Research, 51, 79–93.

Sheldrick, G.M. (2008) A short history of *SHELX*. Acta Crystallographica, A64, 112–122.

Villar, E., Cabrol, L., and Heimbürger-Boavida, L.-E. (2020) Widespread microbial mercury methylation genes in the global ocean. Environmental Microbiology Reports, 12, 277–287.

Figure Captions

Figure 1. (**a**) Reflective silvery black interpenetrating mikecoxite laminae on quartz. (**b**) Dispersed elongated blades of mikecoxite on and in pale-orange kleinite and on quartz. Scale bar = 50 μm. (photo: Michael Cox, Keyence VHX-970, VHZ-100T lens).

Figure 2. Raman spectrum of mikecoxite.

Figure 3. Electron-microprobe wavelength scans for C and O in mikecoxite using LDE1 and LDE2 crystals.

Figure 4. Cation coordination environments for the four Hg sites in the mikecoxite structure. Hg: black, C: gray, O: red, Cl: green circles; strong axial bonds: thick black lines, weak equatorial bonds: thin black lines. Bond lengths in Å.

Figure 5. Anion-coordination environments for the (**a**) C and (**b**) O sites in the mikecoxite structure. Legend as in Fig. 4. Bond-valence contributions to the central anion are in v.u.

Figure 6. The crystal structure of mikecoxite: (**a**) looking onto the [CHg_4OCl] layer, viewed down an axis 10° from [010]; (**b**) looking along the corrugated [CHg_4OCl] layers, stacked along [010] with additional Cl2 atoms residing between layers, viewed down an axis rotated 5° from [001]. Legend as in Fig. 4 with gray-shaded (CHg_4) anion-centered tetrahedra (central layer has (CHg_4) tetrahedra shaded yellow to highlight the individual highly corrugated [CHg_4OCl] layers).

TABLE 1. Chemical analytical data (wt%) for mikecoxite.

	Mean	Min.	Max.	S.D.	Probe Standard	[SREF]*
Hg	86.38	79.70	91.60	3.58	HgTe	88.84
Cl	11.58	9.60	15.20	1.79	NaCl	7.69
Br	0.46	0.23	0.66	0.14	KBr	0.37
O**						1.77
C	1.81	1.58	1.95	0.20	Hg-acetate	1.33
Total	100.23					

* values are based on the refined crystal-structure.
** The peak of the O*K*α line (Fig. 3) is too weak to quantify the amount of O in the EMP analysis.

TABLE 2. Powder X-ray diffraction data (*d* in Å) for mikecoxite. Only calculated lines with $I > 2.5$ are listed.

I_{obs}	d_{obs}	d_{calc}	I_{calc}	*h k l*
34	5.49	5.5056	13	-1 0 1
		5.5024	15	1 0 1
		5.2450	3	0 2 0
14	4.89	4.8750	6	-1 1 1
		4.8727	5	1 1 1
32	4.65	4.6610	25	1 2 0
		4.5735	3	2 1 0
16	4.10	4.0934	7	0 2 1
22	3.746	3.7503	7	-2 1 1
		3.7483	7	2 1 1
		3.3065	5	1 3 0
19	3.226	3.2240	14	3 1 0
		3.1873	3	2 2 1
81	2.989	3.0098	10	-3 0 1
		3.0082	10	3 0 1
		2.9874	20	-1 1 2
		2.9864	24	1 1 2
		2.9517	9	-1 3 1
		2.9512	9	1 3 1
100	2.884	2.8807	100	2 3 0
		2.7770	7	0 2 2
14	2.759	2.7528	9	-2 0 2
		2.7512	5	2 0 2
79	2.673	2.6792	24	-1 2 2
		2.6785	22	1 2 2
		2.6626	15	-2 1 2
		2.6612	17	2 1 2
		2.6371	3	-2 3 1
		2.6364	3	2 3 1
19	2.537	2.5410	21	4 0 0
		2.5393	3	1 4 0
		2.4696	8	4 1 0
		2.3674	3	1 4 1
		2.3305	5	2 4 0
30	2.300	2.2977	15	-3 1 2
		2.2963	14	3 1 2
10	2.1429	2.1483	3	-3 2 2
		2.1472	4	3 2 2
30	2.0453	2.0467	17	0 4 2
18	2.0096	2.0066	7	-1 4 2
		2.0063	6	1 4 2
		1.9957	3	5 1 0
11	1.9738	1.9772	3	-3 4 1
		1.9768	3	3 4 1
		1.8954	6	5 2 0
9	1.8286	1.8352	3	-3 0 3
		1.8341	3	3 0 3
		1.8216	3	-1 3 3
		1.8212	3	1 3 3
		1.7837	4	3 5 0
40	1.7443	1.7483	10	0 6 0
		1.7412	12	-4 3 2
		1.7404	10	4 3 2
		1.7402	3	1 5 2
10	1.6970	1.6976	5	-5 3 1
		1.6971	5	5 3 1
		1.6891	3	0 6 1
26	1.6379	1.6407	5	-5 2 2
		1.6399	5	5 2 2
		1.6368	12	0 0 4
		1.6066	3	5 4 0
7	1.5975	1.5943	4	-4 4 2
		1.5936	5	4 4 2
11	1.5657	1.5665	6	-3 5 2
		1.5660	6	3 5 2
		1.5245	3	6 3 0
11	1.5049	1.5049	6	-6 0 2
		1.5041	5	6 0 2
12	1.4405	1.4403	4	4 6 0
		1.4383	3	7 1 0
27	1.4222	1.4233	10	-2 3 4
		1.4230	5	6 4 0
		1.4229	12	2 3 4

TABLE 3. Data collection and structure-refinement details for mikecoxite.

Diffractometer	Bruker D8 three-circle; multilayer optics; APEX-II
CCD X-ray radiation / source	Mo*K*α (λ = 0.71073 Å) / rotating anode
Temperature	293(2) K
Refined formula	$[CHg_4]O(Cl_{1.958}OBr_{0.042})_{\Sigma 2}$
Space group	$P2_1/n$
Unit cell dimensions	a = 10.164(5) Å
	b = 10.490(4) Å
	c = 6.547(3) Å
	β = 90.037(10)°
V	698.0(5) $Å^3$
Z	4
Density (calculated)	8.594 $g{\cdot}cm^{-3}$
Absorption coefficient	88.59 mm^{-1}
F(000)	1475
Crystal size	10 x 15 x 25 μm
θ range for data collection	2.79 to 30.07°
Index ranges	$-14 \le h \le 14$, $-14 \le k \le 14$, $-9 \le l \le 9$
Reflections collected	23355
Ewald reflections	8174
Unique reflections	2055 [R_{merge} = 0.016]
Reflections with Io > 2σI	1774
Completeness to θ = 30.07°	100 %
Refinement method	Full-matrix least-squares on F^2
Parameters / restraints	75 / 0
Goodness-of-fit on F2	1.064
Final R indices [Io > 2σI]	R_1 = 0.0180, wR_2 = 0.0453
R indices (all data)	R_1 = 0.0243, wR_2 = 0.0483
Absolute structure parameter	0.44(8)
Largest diff. peak and hole	1.85 and –1.73 e/A^3

*$R_{int} = \Sigma|F_o^2 - F_o^2(\text{mean})| / \Sigma[F_o^2]$; GoF = $S = \{\Sigma[w(F_o^2 - F_c^2)^2] / (n-p)\}^{1/2}$; $R1 = \Sigma||F_o| - |F_c|| / \Sigma|F_o|$; $wR_2 = \{\Sigma[w(F_o^2 - F_c^2)^2] / \Sigma[w(F_o^2)^2]\}^{1/2}$; $w = 1/[\sigma^2(F_o^2) + (aP)^2 + bP]$ where a is 0.0293, b is 0.6145 and P is $[2F_c^2 + \text{Max}(F_o^2,0)]/3$.

TABLE 4. Atom positions, occupancy and displacement parameters (Å)^2 for mikecoxite.

Site	Occupancy	*x*/*a*	*y*/*b*	*z*/*c*	U_{eq}
Hg1	Hg	0.40677(2)	0.05330(2)	0.24980(8)	0.02782(7)
Hg2	Hg	0.10095(2)	0.24087(2)	0.25532(6)	0.02346(6)
Hg3	Hg	0.84448(6)	0.09441(6)	0.50243(5)	0.02318(17)
Hg4	Hg	0.84393(6)	0.09377(6)	0.00871(5)	0.02367(17)
O	O	–0.0248(5)	0.0835(4)	0.2587(15)	0.0218(10)
C	C	0.7229(6)	0.1017(6)	0.753(2)	0.0242(13)
Cl1	Cl	0.55343(16)	0.22760(16)	0.2540(6)	0.0308(3)
Cl2	$Cl_{0.958}Br_{0.042(6)}$	0.34116(18)	0.11223(16)	0.7441(8)	0.0418(7)

	U^{11}	U^{22}	U^{33}	U^{23}	U^{13}	U^{12}
Hg1	0.02534(12)	0.02904(13)	0.02908(12)	0.0003(3)	–0.0009(4)	–0.00320(9)
Hg2	0.02141(11)	0.02696(11)	0.02203(11)	0.0005(3)	0.0001(3)	–0.00213(9)
Hg3	0.0219(4)	0.0279(4)	0.0198(2)	–0.00027(13)	0.0017(2)	0.0004(2)
Hg4	0.0217(4)	0.0295(4)	0.0197(2)	0.00027(14)	–0.0013(2)	0.0003(2)
O	0.025(2)	0.026(2)	0.014(2)	0.009(4)	0.007(4)	0.0021(17)
C	0.022(3)	0.030(3)	0.021(3)	0.009(5)	–0.004(6)	–0.003(2)
Cl1	0.0307(7)	0.0299(7)	0.0318(8)	0.0038(16)	–0.0016(14)	–0.0028(6)
Cl2	0.0309(9)	0.0362(10)	0.0584(14)	0.0034(18)	0.010(2)	–0.0017(7)

TABLE 5. Selected interatomic distances (Å) and angles (°) for the [CHg_4OCl] layer in mikecoxite.

C–Hg1	2.093(6)	Hg1–Cl1	2.3592(18)	C–Hg1–Cl1	179.7(4)
C–Hg2	2.065(6)	Hg2–O	2.088(5)	C–Hg2–O	179.1(2)
C–Hg3	2.054(13)	Hg3–O	2.080(8)	C–Hg3–O	177.1(3)
C–Hg4	2.080(13)	Hg4–O	2.114(9)	C–Hg4–O	177.0(3)
<C–Hg>	2.073				
Hg1–C–Hg2	104.1(3)	Hg2–O–Hg3	110.8(4)		
Hg1–C–Hg3	110.1(5)	Hg3–O–Hg4	100.8(2)		
Hg1–C–Hg4	110.3(5)	Hg2–O–Hg4	109.7(3)		
Hg2–C–Hg3	113.4(5)	<Hg–O–Hg>	107.1		
Hg2–C–Hg4	112.3(6)				
Hg3–C–Hg4	106.6(3)				
<Hg–C–Hg>	109.5				

1

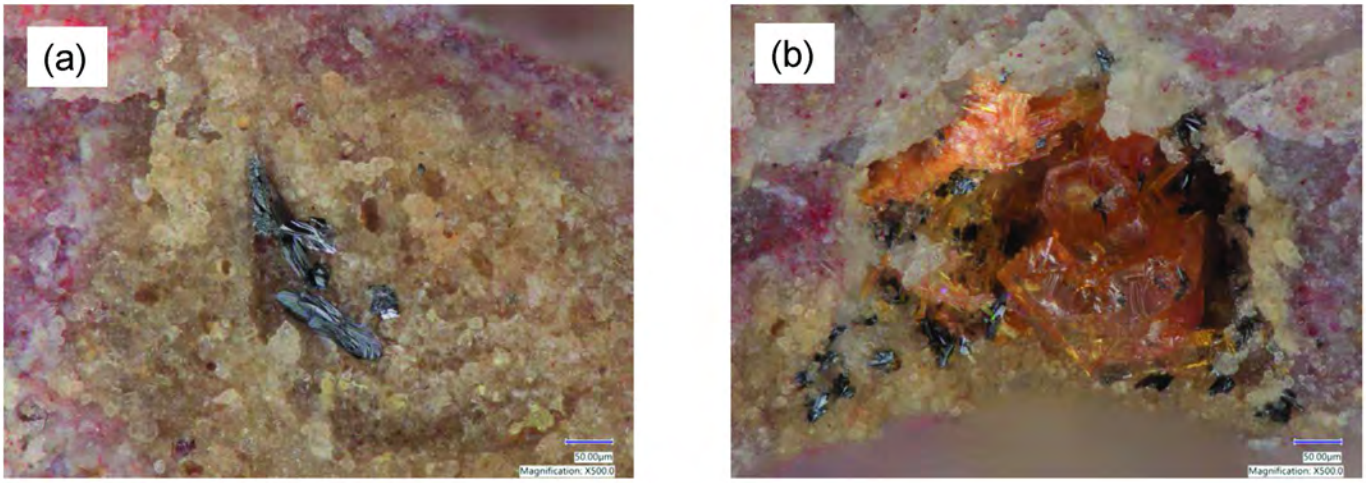
(a)
50.00µm
Magnification: X500.0
(b)
50.00µm
Magnification: X500.0

2

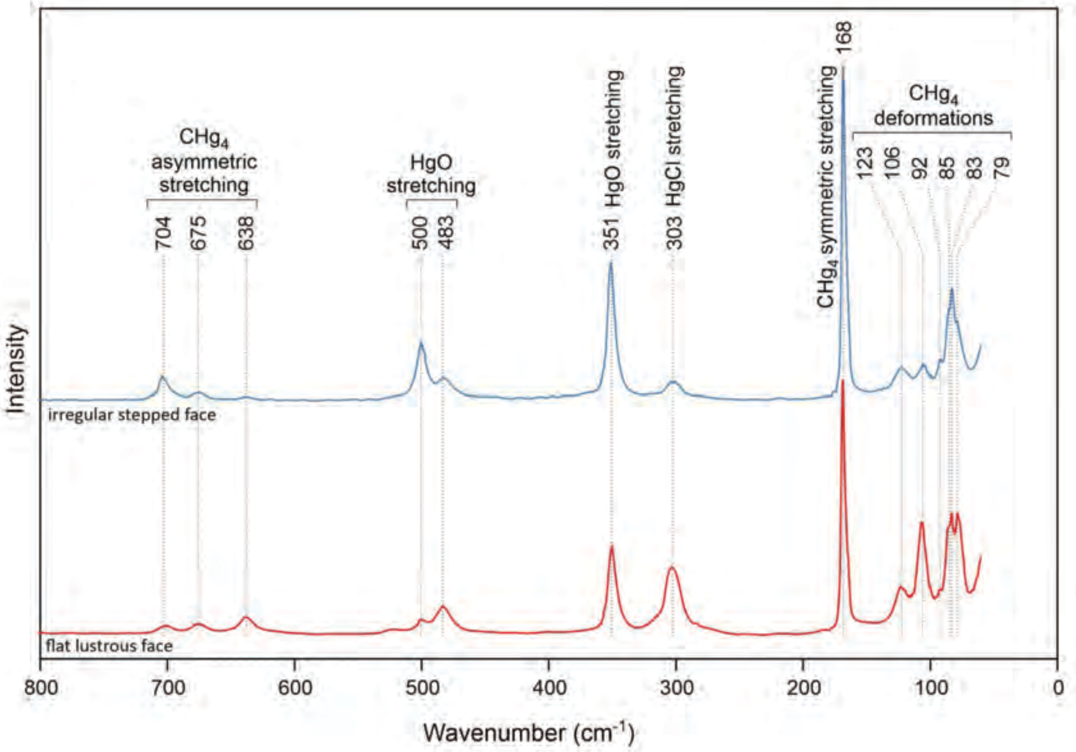
CHg$_4$ asymmetric stretching
704
675
638
HgO stretching
500
483
351 HgO stretching
303 HgCl stretching
CHg$_4$ symmetric stretching
168
CHg$_4$ deformations
123
106
92
85
83
79
Intensity
irregular stepped face
flat lustrous face
800
700
600
500
400
300
200
100
0
Wavenumber (cm^{-1})

3

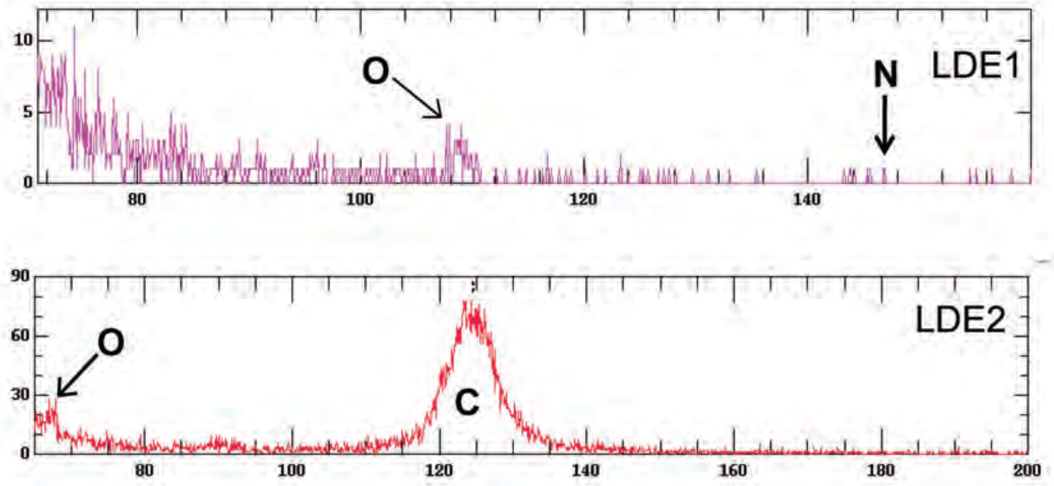
10
5
0
80
100
120
140
O
N
LDE1
90
60
30
0
80
100
120
140
160
180
200
O
C
LDE2

4

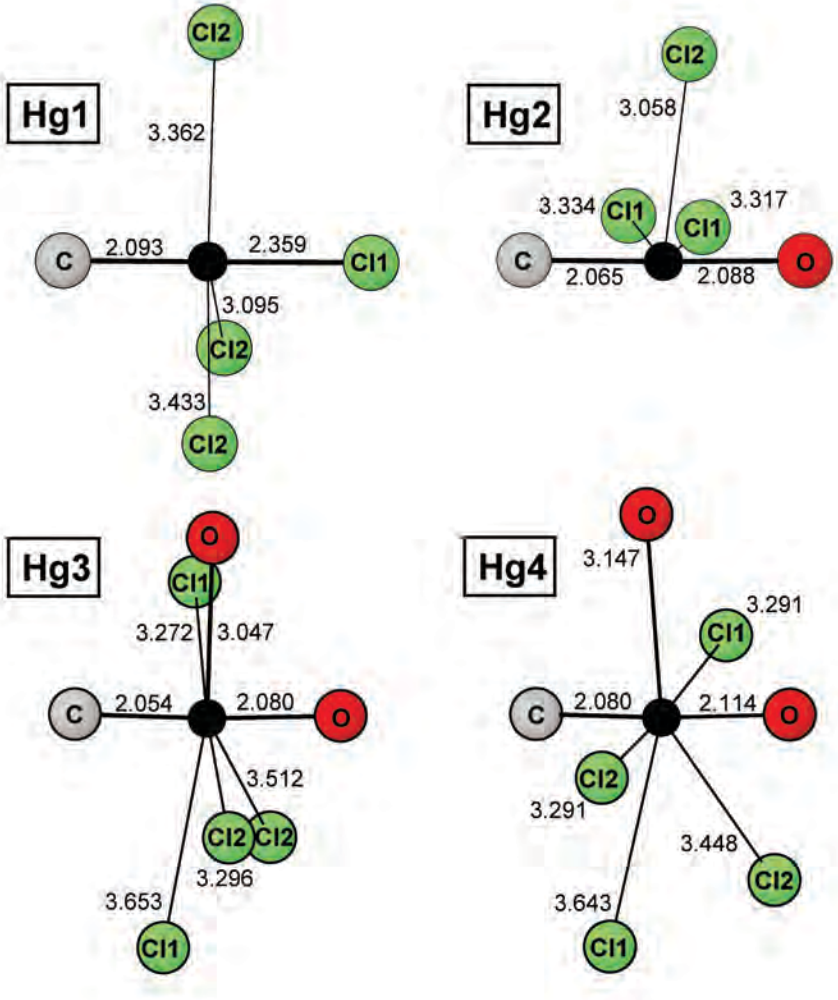
Hg1
Cl2
3.362
C
2.093
2.359
Cl1
3.095
Cl2
3.433
Cl2
Hg2
Cl2
3.058
3.334
Cl1
3.317
Cl1
C
2.065
2.088
O
Hg3
O
Cl1
3.272
3.047
C
2.054
2.080
O
3.512
Cl2
Cl2
3.296
3.653
Cl1
Hg4
O
3.147
3.291
Cl1
C
2.080
2.114
O
Cl2
3.291
3.448
Cl2
3.643
Cl1

5

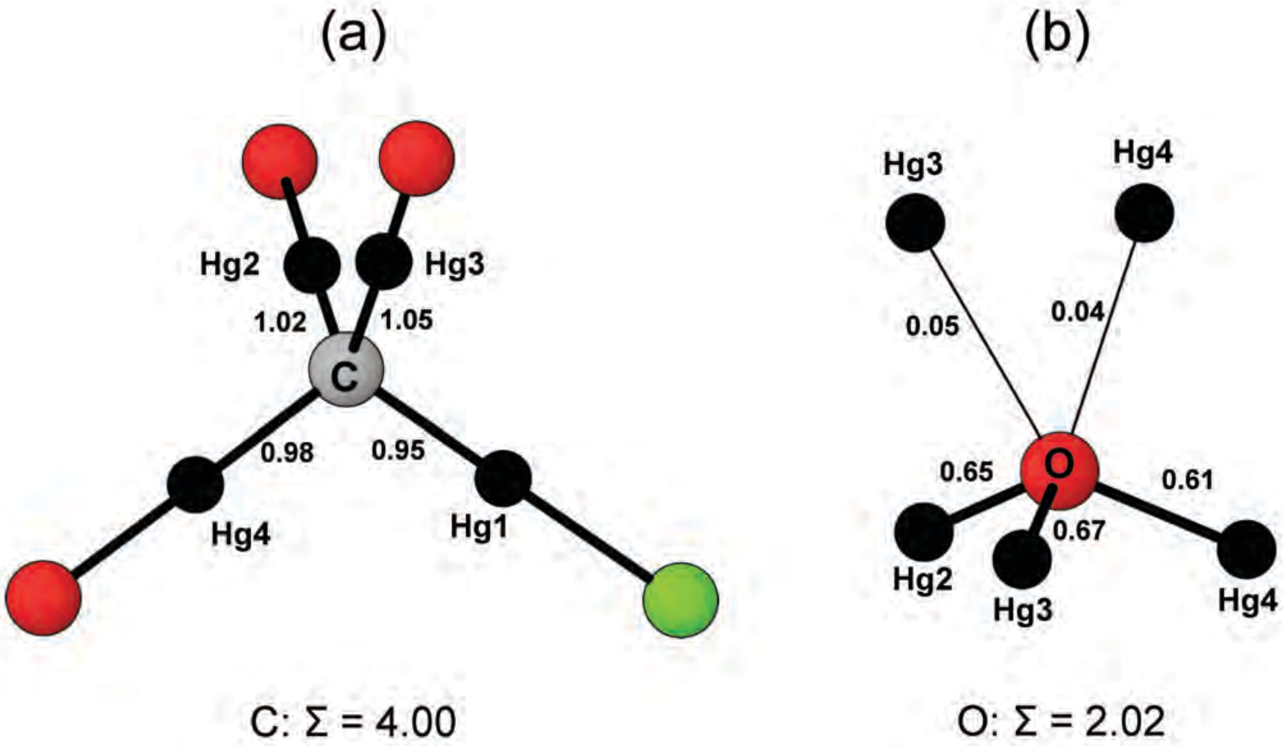
(a)
Hg2
Hg3
1.02
1.05
C
0.98
0.95
Hg4
Hg1
C: Σ = 4.00
(b)
Hg3
Hg4
0.05
0.04
0.65
O
0.61
0.67
Hg2
Hg3
Hg4
O: Σ = 2.02

6